

Sirry MS, Davies NH, Kadner K, Dubuis L, Saleh MG, Meintjes EM, Spottiswoode BS, Zilla P, Franz T. Micro-structurally detailed model of a therapeutic hydrogel injectate in a rat biventricular cardiac geometry for computational simulations. *Comput Methods Biomech Biomed Eng*, 2013, In press

## RESEARCH ARTICLE

# Micro-structurally detailed model of a therapeutic hydrogel injectate in a rat biventricular cardiac geometry for computational simulations

Mazin S. Sirry<sup>a</sup>, Neil H. Davies<sup>a</sup>, Karen Kadner<sup>a</sup>, Laura Dubuis<sup>a</sup>, Muhammad G. Saleh<sup>b</sup>, Ernesta M. Meintjes<sup>b</sup>, Bruce S. Spottiswoode<sup>b,c</sup>, Peter Zilla<sup>a</sup> and Thomas Franz<sup>a,d,e,f,\*</sup>

<sup>a</sup>Cardiovascular Research Unit, Chris Barnard Division of Cardiothoracic Surgery, University of Cape Town, Observatory, South Africa

<sup>b</sup>MRC/UCT Medical Imaging Research Unit, Department of Human Biology, University of Cape Town, Observatory, South Africa

<sup>c</sup>Department of Radiology, Stellenbosch University, Tygerberg, South Africa

<sup>d</sup>Programme for the Enhancement of Research Capacity, Research Office, University of Cape Town, Mowbray, South Africa

<sup>e</sup>Centre for Research in Computational and Applied Mechanics, University of Cape Town, Rondebosch, South Africa

<sup>f</sup>Centre for High Performance Computing, Rosebank, South Africa

\*Send correspondence to:  
Thomas Franz, PhD  
Cardiovascular Research Unit  
Faculty of Health Sciences  
University of Cape Town  
Private Bag X3  
7935 Observatory  
South Africa  
Tel: +27 21 406 6418  
Fax: +27 21 448 5935  
E-mail: [thomas.franz@uct.ac.za](mailto:thomas.franz@uct.ac.za)

## **Abstract**

Biomaterial injection based therapies have showed cautious success in restoration of cardiac function and prevention of adverse remodelling into heart failure after myocardial infarction (MI). However, the underlying mechanisms are not well understood. Computational studies utilised simplified representations of the therapeutic myocardial injectates. Wistar rats underwent experimental infarction followed by immediate injection of polyethylene glycol hydrogel in the infarct region. Hearts were explanted, cryo-sectioned and the region with the injectate histologically analysed. Histological micrographs were used to reconstruct the dispersed hydrogel injectate. Cardiac magnetic resonance imaging (CMRI) data from a healthy rat were used to obtain an end-diastolic biventricular geometry which was subsequently adjusted and combined with the injectate model. The computational geometry of the injectate exhibited microscopic structural details found the *in situ*. The combination of injectate and cardiac geometry provides realistic geometries for multiscale computational studies of intra-myocardial injectate therapies for the rat model that has been widely used for MI research.

**Keywords:** myocardial infarction; therapeutic injectate; image-based reconstruction; computational modelling; hydrogel

## 1 Introduction

In 2002, 16.7 million people died from cardiovascular diseases worldwide, nearly half of which were attributed to coronary heart disease (AHA 2008). An estimated 80.7 million American adults (one in three) had one or more types of cardiovascular disease in 2005. About half (50.6%) of 16 million people with coronary heart disease were recuperating from myocardial infarction (MI). Up to one third of MI patients develop heart failure, a condition currently affecting 5.3 million people, making MI the most common cause of heart failure (HF) (WHO 2008).

Whilst heart failure after MI can be stabilized with treatment regimens based on angiotensin-converting enzyme inhibitors, angiotensin receptor blockers and  $\beta$ -blockers, in the majority of cases HF still advances, though its progression may be slowed (Jessup et al. 2009). The early adaptive response after an ischemic event results in an increase in left ventricular (LV) cavity volume that augments contractility through the Frank-Starling mechanism (Katz 2009) and causes an elevation of wall stress. It is widely postulated that the increase in wall stress is a major cause of the initial positive adaptation of the heart post-MI to turn pathological (Opie et al. 2006). The only efficacious treatment currently available is heart transplantation, which however suffers from a chronic shortage of organ donations.

Extensive research has been undertaken to develop new MI treatments for prevention or inhibition of adverse remodelling of the heart that often culminates in heart failure (Guccione et al. 2003; Klodell Jr et al. 2008). Cell therapy aiming at regeneration of the injured tissue has been one therapy approach (Kawamoto et al. 2003; Mangi et al. 2003; Tomita et al. 2002). The delivery is based on embedding the cells in a carrier medium that is injected into the infarcted myocardium. Restoration or improvement of the pump function of the infarcted heart was indeed observed with this approach (Christman et al. 2004a; Christman et al. 2004b; Ifkovits et al. 2010; Kofidis et al. 2005; Landa et al. 2008; Nelson et al. 2011; Ruvinov et al. 2011). It is, however, not well understood whether the beneficial effects have been a result of the cellular signalling,

causing myocardial regeneration or decreased apoptosis, the mechanical effects of increasing the LV wall thickness or a combination of both.

In attempts to improve the understanding of the underlying mechanisms, computational models have been utilized to study the mechanical effects of the injection of biomaterials into the heart. Wall et al. (2006) investigated injections into infarct zone and border zone with various injection volumes (0.5-5% of total myocardial volume) and a range of mechanical properties of the injectable biomaterial. The injectates were represented by local adjustment of the finite element mesh. The most important outcome of this study for acellular and cellular MI therapy approaches was that small amounts of injected biomaterial can alter cardiac mechanics, reduce wall stress and affect cardiac performance. Wenk et al. (2009) developed a method to optimize the pattern of multiple injection of a polymeric biomaterial. The results indicated an intuitive injection pattern with the greatest number of inclusions when aiming at minimising the mean end-diastolic and end-systolic myofibre stress but ignoring LV stroke volume. A non-intuitive pattern was, however, found as optimum when both myofibre stress and stroke volume were considered. Wenk et al. (2011) investigated the treatment of an LV infarct with the injection of a calcium hydroxyapatite-based tissue filler and demonstrated an increase of ejection fraction and a reduction of end-diastolic and end-systolic fibre stress in the remote and infarct regions for the treated case compared to the untreated case. These three studies demonstrated benefits that can be derived from computational models for the improvement of MI therapies utilizing myocardial injections. However, the biomaterial injectates were simulated either in a 'smearing' approach by adjusting wall thickness and constitutive properties of the region of injection but without geometrically representing the injectate (Wall et al. 2006; Wenk et al. 2011) or in injectate patterns difficult to be achieved *in vivo* (Wenk et al. 2009). More recently, Kortsmits et al. (2012) implemented in computational models the discrete layer-wise configurations of the myocardial injectate to emulate, also still simplified, striated injectate distributions observed *in vivo* (Dobner et al. 2009; Ifkovits et al. 2010; Kadner et al. 2012).

In the present study, we investigated the distribution of polyethylene glycol (PEG) gel injections in infarcted myocardium in the rat model. Using histological methods, microscopic imaging and computational reconstruction, the three-dimensional geometry of a hydrogel injectate in the infarcted myocardial region of the LV was obtained. Particular emphasis was placed on a high spatial resolution of the injectate to enable a realistic representation in computational models both at macroscopic and microscopic level. In combination with the reconstruction of a rat biventricular cardiac geometry from CMRI data, a combined three-dimensional model of a rat heart with left ventricular biomaterial injectate was obtained.

## **2 Materials and methods**

### ***2.1 PEG preparation and labelling***

Vinyl sulfone (VS) functionalized PEG gels (20kDa, 8arm) were manufactured as described by Dobner et al. (Dobner et al. 2009). Per gel, 1  $\mu$ l of 10mg/ml Alexa Fluor® 660 C2 maleimide (Invitrogen Molecular Probes, Eugene, Oregon, USA) in dimethyl sulfoxide (DMSO, Sigma-Aldrich Chemie GmbH, Steinheim, Germany) was added to 1  $\mu$ l of 15.4 mg/10 ml dithiothreitol (DTT, Sigma-Aldrich Chemie GmbH, Steinheim, Germany) in iso-osmotic phosphate-buffered saline (iPBS, 0.15M, pH 7.5) and reacted for 30 min at 37°C. Gels of 10% (m/v) nominal concentration were prepared by dissolving 10 mg of 20 PEG-8VS in 25  $\mu$ l iPBS and adding 1  $\mu$ l of the above Alexa/DTT solution. The pre-polymer was cross-linked with 3.45 mg MMP-1 degradable peptide (GenScript USA Inc., Piscataway, NJ, USA) in 75 $\mu$ l iPBS, then aspirated into a syringe and injected into the myocardium before the components were able to polymerize.

## ***2.2 Induction of myocardial infarct and injection of PEG hydrogel***

The animal experiments were approved by the Institutional Review Boards of the University of Cape Town and performed in accordance with the National Institutes of Health (NIH, Bethesda, MD, USA) guidelines. Surgical procedures were performed according to Huang et al. (Huang et al. 2006). In brief, male Wistar rats (180-220g) were anaesthetized with a mix of oxygen and 5.0% Isoflurane (Safeline Pharmaceuticals (Pty) Ltd., Johannesburg, South Africa), intubated with a 16G intravenous catheter (B. Braun Melsungen AG, Melsungen, Germany) and placed onto a heated operating board (Braintree Scientific, Inc., Braintree, MA, USA). Throughout surgery the animals were ventilated (112 breaths/min) while anaesthesia was maintained with a mix of oxygen/2.0% isoflurane. The heart was exposed via left thoracotomy performed along the 4<sup>th</sup> intercostal space. After pericardiotomy, myocardial infarction was induced by permanent ligation of the left anterior descending coronary artery with a 6-0 non-absorbable polypropylene ligature (Ethicon Inc., Somerville, NJ, USA) 3 mm distal the auricular appendix. Discolouration of the anterior ventricular wall and reduced contractility were hallmarks of a successful occlusion of the artery. Immediately after infarct induction, animals received 100 µl 20PEG-8VS cross-linked with MMP1-degradable peptide via injection into the infarcted area of the myocardium. After allowing for dispersion and in situ polymerization of the PEG gel for 30 min, animals were humanely killed. The hearts were carefully harvested, thoroughly rinsed with saline (Adcock Ingram Critical Care, Johannesburg, South Africa).

## ***2.3 Tissue processing, sectioning and histological image acquisition for injectate reconstruction***

The hearts were mounted onto chucks and snap frozen in liquid nitrogen (Air Liquide (Pty) Ltd, Germiston, South Africa). Sectioning was performed on a cryostat (Microm, Heidelberg, Germany) from the apex towards the base of the heart, taking two adjacent 30µm sections at 20

levels with an inter-level distance of 200 $\mu$ m. Sections were dipped into phosphate buffered saline and mounted using DAPI mount (Vector Laboratories, Burlingame, CA, USA).

Microscopic images were acquired with an Eclipse 90i Fluorescent Microscope with digital camera DXM-1200C and fluorescein isothiocyanate (FITC) filter (all Nikon Corporation, Tokyo, Japan) at 3.2x magnification and stitched (NIS Elements BR 3.0, Nikon, Corporation, Tokyo, Japan) to obtain composite images of the entire short-axis cross section of the heart at each level.

#### **2.4 Geometrical reconstruction of myocardial injectate**

Histological images of the heart closest representing the observation in our previous studies (Dobner et al. 2009; Kadner et al. 2012) were utilised for reconstruction. Short-axis cross section composite images of 20 histological sections in cardiac longitudinal direction were imported in Adobe Photoshop CS3 (Adobe Systems Inc, San Jose, CA, USA), stacked and aligned to represent the *in vivo* configuration. The region containing the PEG gel was cropped in each image and the resulting image stack imported in Simpleware (Simpleware Ltd., Exeter, UK). The appropriate in plane resolution and the section-to-section distance were defined by setting the x, y and z spacing parameters to 0.002, 0.002 and 0.245 mm, respectively. The x and y spacing values were acquired from a calibration scale image captured at 3.2x magnification whereas the z spacing value was obtained from the level distance of the cryo-sectioning process. Image noise and artefacts were reduced using bilateral filters. 2D spatial segmentation masks were developed for the gel injectate in the individual images using region-growing segmentation algorithms. Through stacking of these 2D masks, a 3D geometric model of the PEG gel was developed.

#### **2.5 Reconstruction of biventricular cardiac geometry**

Cardiac magnetic resonance (CMR) images obtained from a healthy rat using a custom built transmit-receive small-animal bird cage coil with 70 mm diameter in a 3.0T Magnetic Resonance

Imaging (MRI) system (Allegra, Siemens Healthcare, Erlangen, Germany) were utilized to reconstruct a 3D biventricular geometry of a rat heart. Short axis cine images were acquired using an ECG and respiratory gated cine FLASH sequence with the following parameters; TR/TE: 7.7/3.5 ms, resolution:  $0.234 \times 0.234 \times 1 \text{ mm}^3$ , flip angle:  $25^\circ - 40^\circ$ , number of signal averages (Saleh et al. 2012).

An end-diastolic short-axis image stack was imported in Simpleware utilising spatial parameters encoded in the MR images. Gradient anisotropic diffusion and gradient magnitude filters were employed to reduce image noise and enhance the appearance of endocardial and epicardial contours. 2D spatial masks of the myocardium were developed using a combination of intensity thresholding and region growing segmentation algorithms. The 2D masks were stacked and the 3D biventricular end-diastolic geometry was reconstructed.

## 2.6 *Combining cardiac and injectate geometries*

The anterior wall of the LV of the reconstructed cardiac geometry required adjustment to simulate local wall thickening associated with the hydrogel injection. In Simpleware, linear interpolation in z-direction (cardiac longitudinal axis) was performed on the MRI data previously imported and processed for reconstruction of the cardiac geometry. The resulting data exhibited an x-y-z resolution of  $0.234 \times 0.234 \times 0.333 \text{ mm}^3$  to allow for finer smoothing of the geometry adjustments. The wall thickness was increased locally by adjusting the 2D masks of the original and interpolated CMRI slices at the epi- and endo-cardial contours of the LV such that the adjusted cardiac geometry fulfilled the condition:

$$V_{\text{Wall,adj}} \approx V_{\text{Wall}} + V_{\text{Inject}}, \quad (1)$$

where  $V_{\text{Wall,adj}}$  is the wall volume of the adjusted cardiac geometry,  $V_{\text{Wall}}$  is the wall volume of the original cardiac geometry and  $V_{\text{Inject}}$  is the volume of the injectate. The position of these adjustments was matched to the position of the injectate. Subsequently, the reconstructed

injectate geometry was embedded at the predefined injection site in the anterior LV wall of the adjusted cardiac geometry.

### 3 Results

Figure 1(a) shows one histological image of the cross-sectional region of the LV wall with hydrogel gel injectate. Image filtering reduced artefacts and noise in the original acquired histological micrographs (Figure 1b) and the application of the 2D spatial masks enhanced the striations of the gel injectate (Figure 1c). The injectate geometry reconstructed from the set of 20 micrographs is illustrated in Figure 2(a). The microscopic structure obtained for the reconstructed geometry, Figure 2(b), resembled closely the striated micro-structure of the gel injectate observed histologically, see Figure 2(c).

Figure 3(a) shows the set of CMR images at ED time point with contour lines drawn at the epi- and endo-cardial surfaces of the LV (green and red) and RV (aqua and violet). The stages of image processing of each short-axis CMR slice for the 3D reconstruction of the cardiac geometry are illustrated in Figure 3(b-d): The original acquired CMR image (Figure 3b) underwent filtering (Figure 3c) after which a 2D spatial mask was applied (Figure 3d).

The implementation of LV wall thickening at the site of the gel injection is illustrated in Figure 4. Using a 2D mask for the LV, the epi- and endo-cardial contours were adjusted locally (see bottom part of Figure 4) over a distance of 5 mm along the longitudinal axis of the heart. This extension matched the *in situ* height of the injectate of 4.9 mm representing approximately 40% of the distance between apex and base of the rat heart.

The biventricular cardiac geometry as reconstructed from the CMRI data at ED time point is illustrated in Figure 5(a). The reconstructed geometry exhibited a myocardial wall volume of 544 mm<sup>3</sup>. The result of the local adjustments of the anterior LV wall thickness, i.e. bulging at the predefined injection site of the PEG gel, can be observed in Figure 5(b). The wall thickness adjustment increased the total wall volume in the biventricular geometry to 579 mm<sup>3</sup>. The

combined model with the PEG gel geometry embedded in the cardiac geometry at the injection site is illustrated in Figure 5(c).

## 4 Discussion

Combining histological analysis, CMRI and image-based geometrical reconstruction, we developed a computational biventricular cardiac model of a rat heart with a micro-structurally detailed geometry of a therapeutic PEG hydrogel injectate. The developed geometry of the PEG gel injectate captures the striated distribution of the hydrogel within the myocardium observed *in vivo* in pre-clinical studies when the biomaterial was administered immediately after the infarction (Dobner et al. 2009; Ifkovits et al. 2010; Kadner et al. 2012). With therapeutic myocardial injectates being represented simplified in computational models in previous studies, e.g. by homogenisation (Wall et al. 2006; Wenk et al. 2011) and in coarse layers (Kortsmit et al. 2012), the injectate geometry reconstructed in the current study provides the basis for a more realistic implementation of intra-myocardial injectates in computational models. Due to its micro-structural details, the injectate geometry is particularly suited for the investigation of micro-mechanical interactions between injectate and myocardial tissue. At this microscopic scale, the injectate model may also offer potential for studying the mechanobiology in MI cell therapies for which the injectate provides the physical environment of the injected cells. A macroscopic model of the injectate with less micro-structural details can be obtained from the existing geometry, e.g. to study global mechanics of the heart at reduced computational expense. As such, the models can facilitate multi-scale computational studies into injectate-based MI therapies.

The infarcted rat heart from which the injectate model was developed was explanted minutes after infarct induction. Since geometrical changes were not expected in the cardiac wall during this short period of time, the geometry of the infarcted heart was assumed to be similar to that of

a healthy heart. Accordingly, the biventricular cardiac geometry was developed from cardiac MRI data obtained from a healthy rat.

For the development of computational models, e.g. for finite element analysis, cardiac and injectate geometries need to be complemented with additional structural and constitutive data. Such data can be obtained from literature, such as distribution of myofibre alignment and constitutive properties of the rat heart (Omens et al. 1991) or from experimental tests in case of the injectate biomaterial.

## **5 Conclusions**

The biventricular cardiac rat model combined with an intra-myocardial hydrogel injectate provides realistic geometries for advanced computational investigations into biomaterial-injectate based MI therapies. While the reconstructed injectate geometry stemmed from acellular injections in the rat, an extensively used animal model for MI, the high level of geometrical detail not only allows studying of the injectate-myocardium micromechanics. It can also render the geometry suitable for the representation of the physical environment of cells injected into injured myocardium with the biomaterial and as such promote computational studies of cell mechanics and mechanobiology in MI therapies.

## **Acknowledgements**

This study was supported financially, in part, by the National Research Foundation (NRF) of South Africa, the South African Research Chairs Initiative of the Department of Science and Technology and National Research Foundation of South Africa, the Medical Research Council of South Africa, and NIH Grant no. R21AA017410. Any opinion, findings and conclusions or recommendations expressed in this publication are those of the authors and therefore the NRF

does not accept any liability in regard thereto. MSS acknowledges the International Society of Biomechanics Matching Dissertation Grant.

## **Conflict of Interest Statement**

The authors declare that they have no conflicts of interest in connection with the work presented in this manuscript.

## **References**

- AHA. 2008. Heart disease and stroke statistics: Our guide to current statistics and the supplement to our heart and stroke facts. Dallas: American Heart Association.
- Christman KL, Fok HH, Sievers RE, Fang Q, Lee RJ. 2004a. Fibrin glue alone and skeletal myoblasts in a fibrin scaffold preserve cardiac function after myocardial infarction. *Tissue Eng*, 10(3-4):403-9.
- Christman KL, Vardanian AJ, Fang Q, Sievers RE, Fok HH, Lee RJ. 2004b. Injectable fibrin scaffold improves cell transplant survival, reduces infarct expansion, and induces neovasculature formation in ischemic myocardium. *J Am Coll Cardiol*, 44(3):654-60.
- Dobner S, Bezuidenhout D, Govender P, Zilla P, Davies N. 2009. A synthetic non-degradable polyethylene glycol hydrogel retards adverse post-infarct left ventricular remodeling. *J Card Fail*, 15(7):629-636.
- Guccione JM, Salahieh A, Moonly SM, Kortsmmit J, Wallace AW, Ratcliffe MB. 2003. Myosplint decreases wall stress without depressing function in the failing heart: A finite element model study. *Ann Thorac Surg*, 76(4):1171-80; discussion 1180.
- Huang NF, Sievers RE, Park JS, Fang Q, Li S, Lee RJ. 2006. A rodent model of myocardial infarction for testing the efficacy of cells and polymers for myocardial reconstruction. *Nat Protocols*, 1(3):1596-1609.

- Ifkovits JL, Tous E, Minakawa M, Morita M, Robb JD, Koomalsingh KJ, Gorman JH, Gorman RC, Burdick JA. 2010. Injectable hydrogel properties influence infarct expansion and extent of postinfarction left ventricular remodeling in an ovine model. *Proceedings of the National Academy of Sciences*, 107(25):11507-11512.
- Jessup M, Abraham WT, Casey DE, Feldman AM, Francis GS, Ganiats TG, Konstam MA, Mancini DM, Rahko PS, Silver MA, Stevenson LW, Yancy CW. 2009. 2009 focused update: ACCF/AHA guidelines for the diagnosis and management of heart failure in adults: A report of the american college of cardiology foundation/american heart association task force on practice guidelines: Developed in collaboration with the international society for heart and lung transplantation. *Circulation*, 119(14):1977-2016.
- Kadner K, Dobner S, Franz T, Bezuidenhout D, Sirry MS, Zilla P, Davies NH. 2012. The beneficial effects of deferred delivery on the efficiency of hydrogel therapy post myocardial infarction. *Biomaterials*, 33(7):2060-2066.
- Katz AM. 2009. *Heart failure: Pathophysiology, molecular biology and clinical management*, Philadelphia, Wolters Kluwer.
- Kawamoto A, Tkebuchava T, Yamaguchi J, Nishimura H, Yoon YS, Milliken C, Uchida S, Masuo O, Iwaguro H, Ma H, Hanley A, Silver M, Kearney M, Losordo DW, Isner JM, Asahara T. 2003. Intramyocardial transplantation of autologous endothelial progenitor cells for therapeutic neovascularization of myocardial ischemia. *Circulation*, 107(3):461-8.
- Klodell Jr CT, Aranda Jr JM, McGiffin DC, Rayburn BK, Sun B, Abraham WT, Pae Jr WE, Boehmer JP, Klein H, Huth C. 2008. Worldwide surgical experience with the paracor heartnet cardiac restraint device. *J Thorac Cardiovasc Surg*, 135(1):188-195.
- Kofidis T, Lebl DR, Martinez EC, Hoyt G, Tanaka M, Robbins RC. 2005. Novel injectable bioartificial tissue facilitates targeted, less invasive, large-scale tissue restoration on the beating heart after myocardial injury. *Circulation*, 112(9 Suppl):I173-7.

- Kortsmit J, Davies NH, Miller R, Macadangdang JR, Zilla P, Franz T. 2012. The effect of hydrogel injection on cardiac function and myocardial mechanics in a computational post-infarction model. *Comput Methods Biomech Biomed Eng*, DOI: 10.1080/10255842.2012.656611.
- Landa N, Miller L, Feinberg MS, Holbova R, Shachar M, Freeman I, Cohen S, Leor J. 2008. Effect of injectable alginate implant on cardiac remodeling and function after recent and old infarcts in rat. *Circulation*, 117(11):1388-1396.
- Mangi AA, Noiseux N, Kong D, He H, Rezvani M, Ingwall JS, Dzau VJ. 2003. Mesenchymal stem cells modified with akt prevent remodeling and restore performance of infarcted hearts. *Nat Med*, 9(9):1195-201.
- Nelson DM, Ma Z, Fujimoto KL, Hashizume R, Wagner WR. 2011. Intra-myocardial biomaterial injection therapy in the treatment of heart failure: Materials, outcomes and challenges. *Acta Biomater*, 7(1):1-15.
- Omens J, May K, McCulloch A. 1991. Transmural distribution of three-dimensional strain in the isolated arrested canine left ventricle. *Am J Physiol Heart Circ Physiol*, 261(3):H918.
- Opie LH, Commerford PJ, Gersh BJ, Pfeffer MA. 2006. Controversies in ventricular remodelling. *Lancet*, 367(9507):356-367.
- Ruginov E, Leor J, Cohen S. 2011. The promotion of myocardial repair by the sequential delivery of IGF-1 and HGF from an injectable alginate biomaterial in a model of acute myocardial infarction. *Biomaterials*, 32(2):565-578.
- Saleh M, Sharp S-K, Alhamud A, Spottiswoode BS, van der Kouwe AJW, Davies NH, Franz T, Meintjes EM. 2012. Long-term left ventricular remodelling in rat model of non-reperused myocardial infarction: Sequential MR imaging using a 3T clinical scanner. *Journal of Biomedicine and Biotechnology*, 2012:10.

Tomita S, Mickle DA, Weisel RD, Jia ZQ, Tumiati LC, Allidina Y, Liu P, Li RK. 2002.

Improved heart function with myogenesis and angiogenesis after autologous porcine bone marrow stromal cell transplantation. *J Thorac Cardiovasc Surg*, 123(6):1132-1140.

Wall ST, Walker JC, Healy KE, Ratcliffe MB, Guccione JM. 2006. Theoretical impact of the injection of material into the myocardium - a finite element model simulation. *Circulation*, 114(24):2627-2635.

Wenk JF, Eslami P, Zhang Z, Xu C, Kuhl E, Gorman Iii JH, Robb JD, Ratcliffe MB, Gorman RC, Guccione JM. 2011. A novel method for quantifying the in-vivo mechanical effect of material injected into a myocardial infarction. *Ann Thorac Surg*, 92(3):935-941.

Wenk JF, Wall ST, Peterson RC, Helgerson SL, Sabbah HN, Burger M, Stander N, Ratcliffe MB, Guccione JM. 2009. A method for automatically optimizing medical devices for treating heart failure: Designing polymeric injection patterns. *J Biomech Eng*, 131(12):121011.

WHO. 2008. The atlas of heart disease and stroke. Geneva: World Health Organization.

## Figures

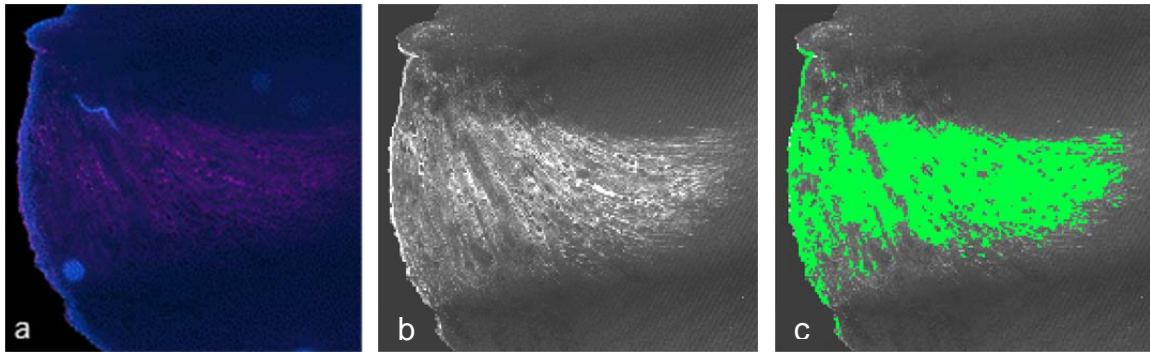


Figure 1. (a) Fluorescent image of the cross-sectional region of the LV wall injected with Alexa Fluor® 660 labelled hydrogel. Nuclei appear blue and hydrogel appears pink. (b) Histology image after conversion to greyscale and image filtering to reduce artefacts and noise. The hydrogel appears white. (c) Selection of the hydrogel and enhancement of the striations by means of a spatial masks appearing in green.

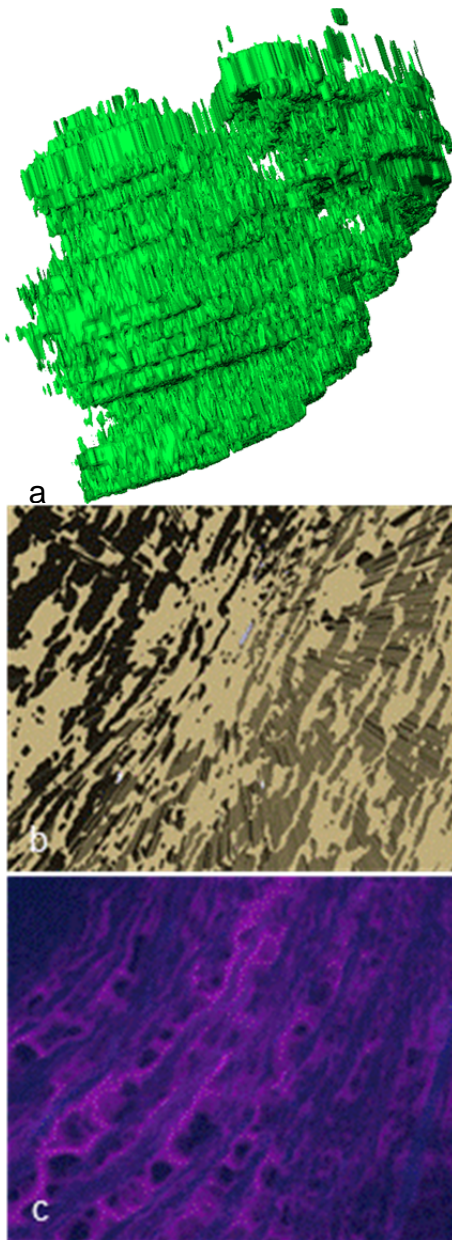


Figure 2. Entire three-dimensional reconstructed injectate geometry (a). A close-up of the injectate geometry (b) reveals that it was feasible to represent the micro-structural striations of the *in situ* hydrogel (c) during the reconstruction process.

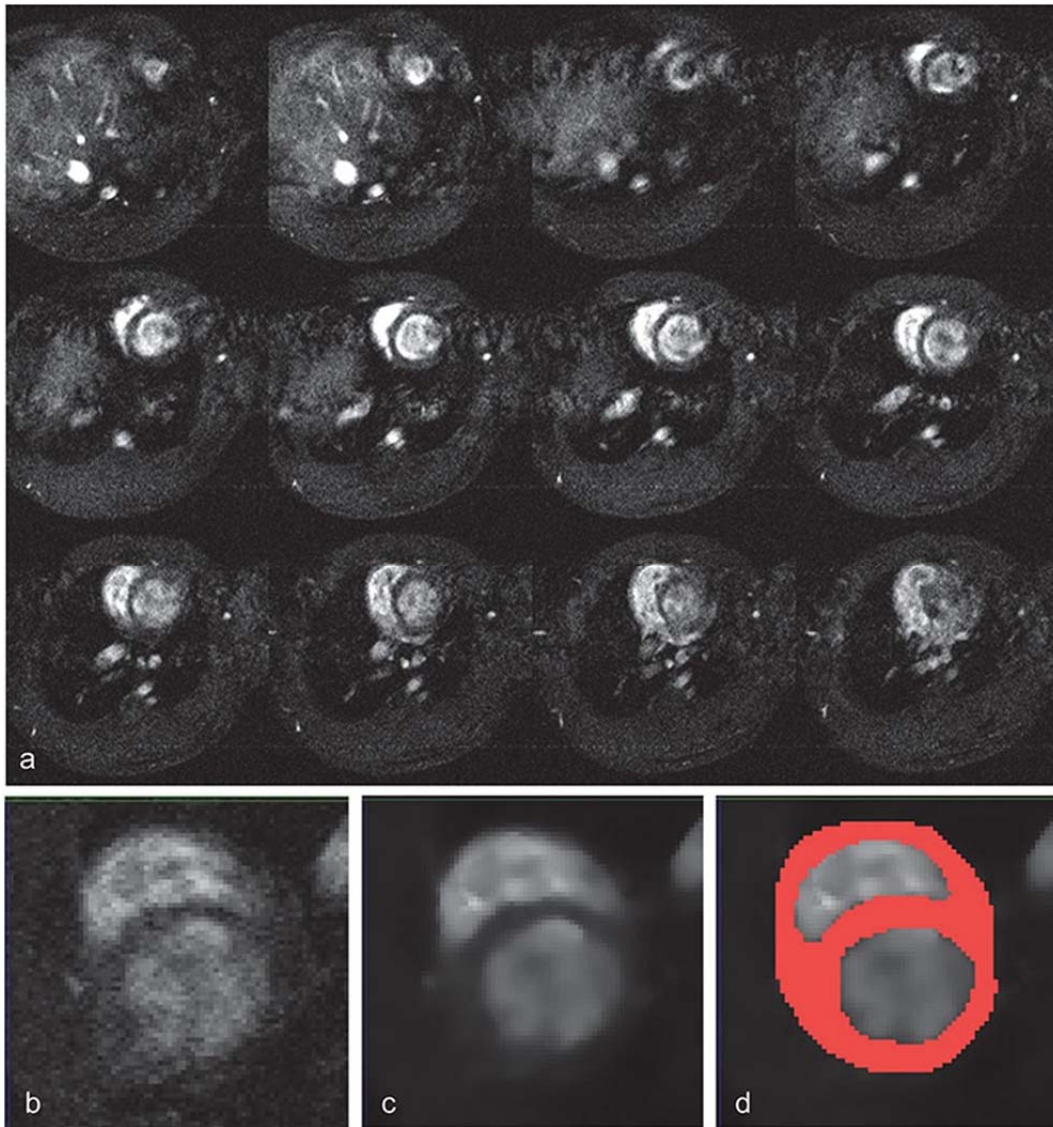


Figure 3. Set of eight MR images of a rat showing short-axis views of the heart at end-diastolic time point. The epi- and endo-cardial contours are delineated in green and red, respectively, for the left ventricle and in aqua and violet, respectively, for the right ventricle (a). Close-up short-axis views of the rat heart from the MR images utilised for geometrical reconstruction: Original image (b), image after filtering for reduction of noise (c), and filtered image with spatial mask identifying the cardiac tissue (d).

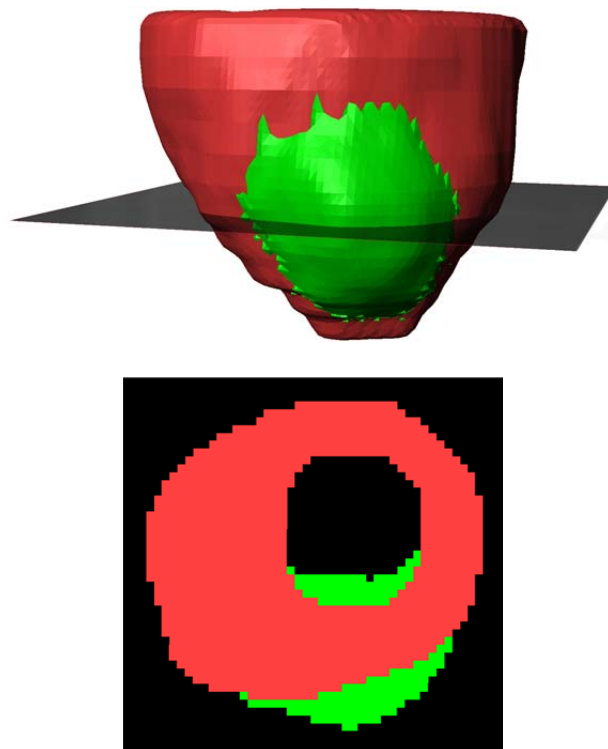


Figure 4. Illustration of the adjustments (in green) of the reconstructed cardiac geometry (in red) to account for the myocardial injectate: Over of 5 mm in cardiac longitudinal direction (top) matching the height of the injectate, the 2D spatial masks in the MR images created for reconstruction of the cardiac geometry were appended locally at epi- and endo-cardial contours (bottom) to generate a local wall thickening of the left ventricle.

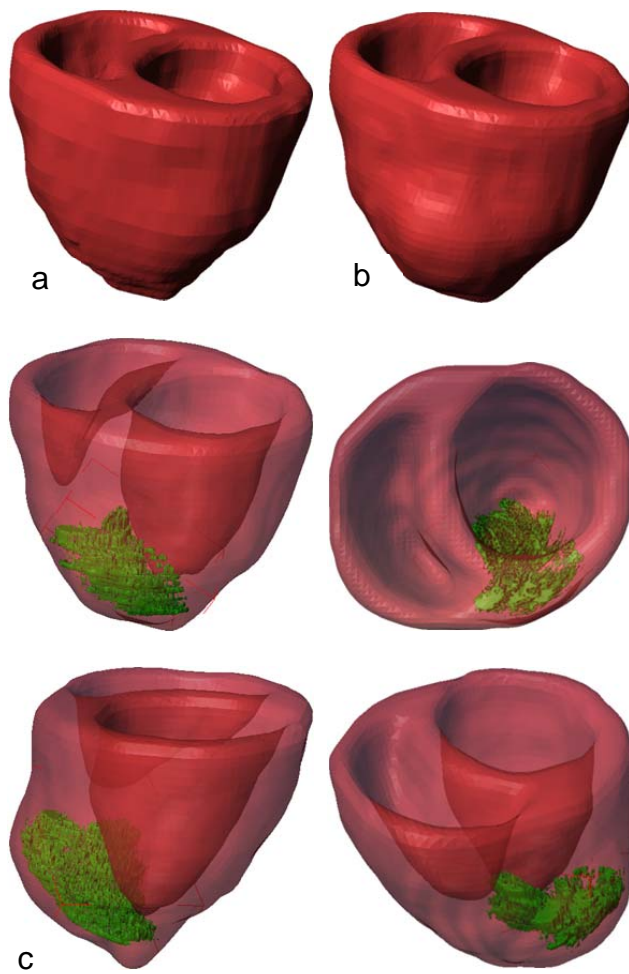


Figure 5. (a) Three-dimensional biventricular geometry of the rat heart reconstructed from MRI data. (b) Biventricular cardiac geometry with local wall thickening to account for the therapeutic myocardial hydrogel injectate. (c) Four views of the adjusted biventricular cardiac geometry combined with reconstructed hydrogel injectate geometry. The cardiac geometry is displayed partially translucent to for illustration purposes.